Int. J. Heat Mass Transfer Vol. 25, No. 6, pp. 759–770, 1982
Printed in Great Britain

0017-9310/82/060759-12 $03.00/0

HOMOGENEOUS NON-EQUILIBRIUM CRITICAL FLOW MODEL

S. LEVY and D. ABDOLLAHIAN
S. Levy, Inc., 1999 S. Bascom Ave., Suite 725, Campbell, CA 95008, U.S.A.

(*Received* 4 *December* 1981)

Abstract—An important aspect of light water reactor safety is the capability to predict the maximum (or critical) mass flow rate from a break or leak in the primary system. During the early stages of such a blowdown, the water is subcooled or slightly saturated and substantial non-equilibrium conditions exist, e.g. the water is superheated above saturation temperature. At present, there is not a single adequate model for critical flow which considers subcooled upstream conditions and thermal non-equilibrium and which is valid for a variety of configurations.

A simplified non-equilibrium flashing model is developed in this report. The model, which is applicable especially to rapidly decreasing pressures along the flow path, presumes that water has to be superheated (or decompressed) a prescribed amount before it starts to flash into steam and that, at a given local pressure below the decompression pressure, enough steam will be formed to bring the water superheat down to the decompression amount. In addition, the flow is assumed to be homogeneous, i.e. the steam and liquid velocities are equal. Finally, an isentropic process is employed to calculate the non-equilibrium steam quality and the critical flow rate.

The proposed flashing model is found to satisfactorily describe the Reocreux [1] and Zimmer *et al.* [2] depressurization and critical flow tests where local pressures and steam void fractions were measured. Overall good agreement is also obtained with the large scale Marviken tests and most other small scale experiments. The model may not be accounting properly for the impact of depressurization rate upon non-equilibrium conditions, and it tends to underpredict small scale tests at high pressures when the contraction zone is not followed by a constant cross-section length.

A key element of the model is the liquid decompression pressure drop or superheat employed in the model. It is shown to be similar to the semi-empirical correlation of Alamgir and Lienhard [3], and a slight modification to their expression is developed based upon the data of Reocreux and Zimmer *et al.*

NOMENCLATURE

A, flow area;
C_c, nozzle irreversible pressure loss coefficient;
D, diameter;
f, friction factor;
G, mass flow rate per unit area;
H, enthalpy;
H_{fg}, heat of vaporization;
k_L, liquid thermal conductivity;
k_S, Boltzmann's constant;
L_c, length after contraction;
N, Henry–Fauske constant;
P, pressure;
Pr, Prandtl number;
S, entropy;
T_c, critical temperature;
T_r, temperature divided by critical temperature;
V^*, critical velocity;
X, steam quality;
X^1, non-equilibrium steam quality;
z, distance along flow direction.

Greek symbols

α, steam volume fraction;
ΔP_d, decompression pressure;
ΔT_d, superheat temperature;
μ, viscosity;
ρ, density;
Σ, depressurization rate;
$\bar{\Sigma}$, average depressurization rate.

Subscripts

c, critical location;
e, entrance;
f, saturated liquid;
FSP, single phase liquid friction;
g, vapor;
L, liquid;
o, stagnation;
max, maximum permitted critical pressure;
p, end of pipe;
s, Ti, saturated at entrance temperature;
t, throat.

INTRODUCTION

DURING a Loss of Coolant Accident (LOCA) in a light water reactor, pressurized water or steam–water will escape from a break or leak in the primary system. The rate of coolant blowdown through the break or leak is most important to the design of Emergency Core Cooling Systems (ECCS) because it determines the depressurization rate and the time to reactor fuel

uncovery. The mass flux discharge depends upon the break or leak configuration, the upstream pressure, and thermodynamic properties, and it tends to be choked and reach a maximum critical flow rate value. Considerable theoretical and experimental studies of critical flow have been reported, and recent reviews have been presented by Abdollahian *et al.* [4] and Saha [5]. The reviews reveal that one particular type of critical flow has escaped full understanding to date. It occurs with subcooled upstream conditions which often produce non-equilibrium thermodynamic conditions (i.e. superheated water) at the point of critical flow. This metastability has been difficult to predict and is much more sensitive to the specific geometric characteristics of the break.

A substantial number of tests and analyses have been attempted of critical flow with subcooled inlet conditions. The experimental studies of Reocreux [1], Sozzi and Sutherland [6], and Zimmer *et al.* [2] are worth highlighting. Also, two analytical models are deserving of note: they are the two-fluid model of Richter [7] and the Henry–Fauske model [8]. The Richter model requires the assumption of an initial bubble diameter (taken between 1×10^{-5} and 1.7×10^{-5} m) and a fixed number of bubble nucleation sites (generally taken at $10^{11}/m^3$). In addition, the analysis specifies the constitutive equations controlling steam–water interface friction and heat transfer for various two-phase flow patterns. While this model has been found to be the most successful in predicting the Marviken tests, it needs adjustments to some of the inputs (e.g. the number of nucleation sites per unit volume must be changed for the Reocreux tests) and it requires extensive computation time. Henry–Fauske utilized a homogenous flow model but assumed that the non-equilibrium steam quality X^1 is proportional to the equilibrium quality X so that

$$X^1 = NX. \tag{1}$$

N was a constant determined empirically from tests and was found to vary with test geometry. In the Marviken tests, N varies from 7 to about 100 in the course of a specific blowdown test.

In this report, we shall develop a simplified flashing process to predict the degree of non-equilibrium. This flashing model combined with the assumptions of isentropic and homogeneous flow is then employed to predict the critical flowrate. In the sections which follow, we shall first discuss the physical characteristics of critical flow under subcooled inlet flow conditions. Next, based upon the observed characteristics, a flashing process will be defined and the critical flow conditions predicted. A comparison of the proposed model with Marviken and other data will follow.

CHARACTERISTICS OF CRITICAL FLOW WITH SUBCOOLED INLET CONDITIONS

Figure 1 illustrates the fluid behavior under critical flow and subcooled upstream conditions. It is taken directly from the tests of Reocreux [1]. Subcooled water at low pressure enters the pipe portion of the test section. As the local pressure, P, decreases along the test section, the saturation pressure, $P_{s,Ti}$, corresponding to the inlet water temperature, Ti, is reached. The water continues to flow along the pipe and becomes superheated until the local pressure P_b provides enough superheat for the first bubble to be formed. Beyond that point, the local pressure continues to decrease until it reaches a value P_d where significant steam begins to be formed.

In Fig. 1, the pressure P_d is reached at the end of the pipe or critical location, or $P_d = P_c$ where P_c is the critical pressure. According to Fig. 1, the steam volume fraction, α, is zero up to the end of the pipe section and increases rapidly beyond that point. At that location, one can define a decompression pressure difference, ΔP_d, below saturation pressure required to form a significant amount of steam, i.e.

$$\Delta P_d = P_{s,Ti} - P_d. \tag{2}$$

In the diffuser section, the local pressure continues to decrease while the steam content and volume fraction increase. From the measured values of local steam fraction α and pressure P, it is possible to calculate a local non-equilibrium steam quality X^1. If one assumes equal steam and water velocity then

$$\frac{X^1}{1 - X^1} = \alpha\rho_g/\rho_L(1 - \alpha) \tag{3}$$

where ρ_g is the vapor density and ρ_L the liquid density. For an isentropic process,* the corresponding liquid entropy, S_L is obtained from

$$S_L = (S_o - X^1 S_g)/(1 - X^1) \tag{4}$$

where S_o is the stagnation entropy and S_g is the saturated steam entropy at the local pressure P. If we assume that the liquid entropy can be evaluated along the saturation line, we can find the saturation pressure, $P + \Delta P_d$, where

$$S_L = S_{f,P+\Delta P_d} \tag{5}$$

and S_f is the saturated water entropy at the pressure, $P + \Delta P_d$. The local decompression pressure drop ΔP_d can then be calculated along the diffuser section and it is plotted on Fig. 1. This calculation reveals that substantial non-equilibrium conditions prevail in the diffuser section and that the decompression pressure difference ΔP_d remains relatively constant and even increases slightly along the diffuser section. Another way to illustrate the degree of non-equilibrium in the pipe and diffuser is to calculate the equilibrium steam quality from an isentropic process, or

$$X = (S_o - S_f)/(S_g - S_f) \tag{6}$$

where S_o is again the stagnation entropy and S_f and S_g are, respectively, the liquid and vapor entropies at the

* A constant stagnation enthalpy process may be more appropriate in the diffuser section and it would give similar answers in this case.

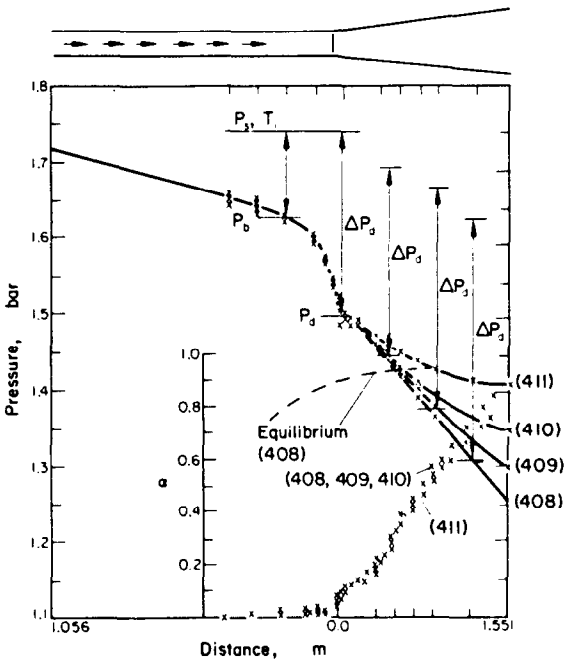

FIG. 1. Characteristics of critical flow with subcooled inlet conditions: Run 408 (Flow 10291. kg/m² s, inlet temp. 115.9°C); Run 409 (Flow 10309. kg/m² s, inlet temp. 115.9°C); Run 410 (Flow 10311. kg/m² s, inlet temp. 115.9°C); Run 411 (Flow 10324. kg/m² s, inlet temp. 116.1°C).

saturation pressure P_s taken equal to the measured local pressure P. The corresponding equivalent volume fraction α_{eq} can be obtained from equation (3) and the results are shown in Fig. 1 by a dashed curve. It is observed again that considerable non-equilibrium conditions prevail prior and after the critical location.

Examination of Fig. 1 leads to several conclusions:

(1) the internal flashing of substantially superheated water to steam is due to decompression and occurs at a pressure P_d which can be quite different from the nucleation pressure P_b of the first bubble. In Fig. 1, nucleated bubbles do not get an opportunity to grow due to the limited time for heat transfer between them and the superheated liquid. Also, the heat transfer rate between steam and water is suspected to be low because their velocities are nearly equal;

(2) as one attempts to decompress water below P_d, some of the water will flash into steam, and the degree of flashing will be such as to bring the water superheat in line with the appropriate decompression pressure drop, ΔP_d, at that location.

Examination of other Reocreux test runs with less inlet subcooling shows that the first formation of steam need not occur at the critical location and that, given enough time, some of the nucleated bubbles may even grow (see Fig. 2). However, the rapid depressurization at the critical location will still produce substantial non-equilibrium at the critical point; and, in fact, calculations there yield relatively the same decompression drop, ΔP_d, as in Fig. 1 if one utilizes the measured values of local steam volume fraction and pressure. Using the decompression pressure drop at the critical point, one can calculate the upstream position where P reaches P_d and significant steam should start to form. The corresponding non-equilibrium steam volume fraction is shown dotted in Fig. 2. The experimental measurements show that, because more time is available in Fig. 2 than in Fig. 1, bubbles nucleated at position P_b tend to grow in Fig. 2. However, as they reach the critical point, they tend to be controlled by the same degree of non-equilibrium produced by ΔP_d.

Because local pressure tends to decrease rapidly close to the critical location, the decompression pressure drop ΔP_d defined in Figs. 1 and 2 can be expected to resemble the decompression pressure drops reported by [9] during rapid static depressurization tests of subcooled water. Alamgir and Lienhard [3] analyzed all the available data for rapid depressurization of subcooled water and proposed the following correlation for ΔP_d

$$\Delta P_d = 0.258\sigma^{3.2}T_r^{13.76}(1 + 13.25\Sigma^{0.8})^{0.5}/(k_s T_c)^{0.5}(1 - \rho_g/\rho_L) \quad (7)$$

where σ is the surface tension, k_s Boltzmann's constant, T_c the critical temperature, Σ the rate of depressurization in Matm/s, T_r the reduced temperature, or the ratio of initial water temperature to critical temperature. For pipe depressurization, Alamgir *et al.* [10] have recommended

$$k_L\Delta T^*/\mu_L(\rho_g/\rho_L)H_{fg} = 1.26/Pr \quad (8)$$

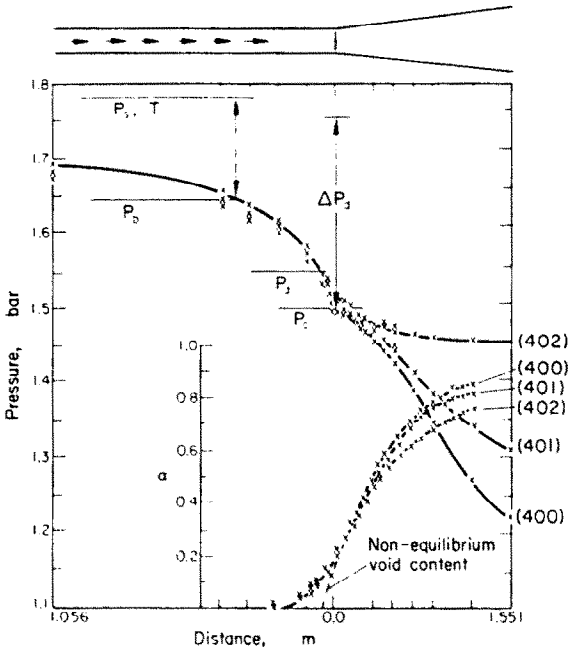

FIG. 2. Characteristics of critical flow with reduced inlet conditions: Run 400 (Flow 6526. kg/m²s, inlet temp. 116.7°C); Run 401 (Flow 6465. kg/m²s, inlet temp. 116.6°C); Run 402 (Flow 6496. kg/m²s, inlet temp. 116.7°C).

where k_L is the liquid thermal conductivity, μ_L the liquid viscosity, H_{fg} the heat of vaporization, Pr the Prandtl number, and ΔT^* is the difference between stagnation temperature and the temperature at the critical location.

In this report, equation (7) is preferred to equation (8) because, as shown later, it makes it possible to account for nozzle configuration through the depressurization term Σ. Also, equation (8) was developed after equation (7) and yields improved predictions at low pressures.

Jones [11] modified equation (7) by trying to take into account the turbulent fluctuations of the flowing liquid. However, a distinction was not made between the two pressures P_b and P_d in Reocreux data in Figs. 1 and 2. Furthermore, the reduction in ΔP_d produced by the fluctuating contribution was calculated by assuming that the fluctuating velocities were each 3σ (3 standard deviations) from the mean fluctuating component.

This fluctuating component is clearly overstated when taken at such a very low probability level for all three velocities simultaneously. This difficulty was alleviated by [12] who sharply reduced the role of turbulent fluctuations in a contracting nozzle and, in fact, utilized equation (7).

Most recently [13] fitted critical flow data by using

$$k_L \Delta T^*/\rho_g V^* H_{fg} D = 5.45/(\rho_L V^* D/\mu_L)^{1.03} \quad (9)$$

where D is the diameter at the critical point and V^* is the critical velocity. Equation (9) reduces to the form of equation (8) if the exponent on the Reynolds number, $\rho_L V^* D/\mu_L$ is taken at 1.0 instead of 1.03.

As noted before, we shall use equation (7) in this report except for adjusting it to match the data of [1] and [2] at low depressurization rates where the validity of equation (7) was not fully checked out.

FLASHING AND CRITICAL FLOW MODEL

The proposed flashing model was formulated from the results discussed under Figs. 1 and 2. It assumes that:

(1) the first significant steam will be formed by flashing when the liquid pressure reaches a prescribed amount ΔP_d below the saturation temperature corresponding to the liquid temperature. At a given instant or location where the pressure is P, the liquid temperature has to be superheated an amount ΔT_d corresponding to ΔP_d along the liquid saturation line for flashing to occur;

(2) if the local pressure continues to decrease below this initial flashing condition, enough water will be converted to steam so that its superheat will again be equal to ΔT_d corresponding to the new pressure P;

(3) any steam formed will be at the saturation conditions corresponding to the pressure P.

If we assume an isentropic flashing process, the non-equilibrium steam quality X^1 is given by

$$X^1 = (S_o - S_L)/(S_g - S_L) \quad (10)$$

where S_o is the stagnation entropy, S_g the saturated vapor entropy at pressure P, and S_L is the

superheated liquid entropy obtained at pressure P and temperature $T + \Delta T_d$ where T is the saturation temperature corresponding to P. By taking the liquid properties along the saturation line, one can write approximately

$$S_L = S_{f,P+\Delta P_d} \quad (11)$$

where S_f is the saturated liquid entropy taken at the saturation pressure of $P + \Delta P_d$.

If one next assumes that the flow is frictionless and is homogeneous, i.e. equal liquid and vapor velocity and that the heat transfer from superheated water to any early nucleated steam bubble is negligible (i.e. no steam presence until the water is decompressed ΔP_d), the energy equation gives

$$H_o = (1 - X^1)H_{f,P+\Delta P_d} + X^1 H_g + (G^2/2\rho^2) \quad (12)$$

where H_o is the stagnation enthalpy, $H_{f,P+\Delta P_d}$ is the saturated liquid enthalpy at the pressure $P + \Delta P_d$, H_g is the vapor enthalpy at the pressure P and G and ρ are the local mass velocity and homogeneous density, corresponding to the non-equilibrium quality X^1.

The critical flow rate is obtained from equations (10)-(12) and a relation for ΔP_d as typified by equation (7). To obtain the critical flow rate, the pressure at the critical location is assumed, the decompression pressure drop ΔP_d is calculated; the non-equilibrium quality is found from equations (10) and (11) and the flow rate computed from equation (12). The critical flow rate, G_c, is determined by finding the critical pressure P_c for which the mass flux, G, is maximum.

It should be realized that two iterations are needed on the parameter ΔP_d. The first one comes about because equation (7) uses the liquid temperature and properties at the liquid temperature. For a prescribed value of the pressure P, the decompression pressure drop, ΔP_d, is first calculated using the stagnation temperature. This first approximation is next used to find the liquid temperature by taking it as the saturation temperature at $P + \Delta P_d$. This new value of liquid temperature is employed to obtain a second approximation to ΔP_d and the liquid temperature and so on until the value of ΔP_d is stabilized.

The second iteration comes about from trying to determine the depressurization rate Σ in equation (7) for accelerating flows. One can write

$$\Sigma = (dP/dt) = (dP/dz)(dz/dt) = (dP/dz)(G/\rho) \quad (13)$$

where z is the distance measured along the flow path and t represents the time.

For a frictionless isentropic fluid, the local pressure gradient with distance z is given by

$$-A\,dP/dz = d(G^2 A/\rho)/dz \quad (14)$$

so that

$$\Sigma = -(G)(G/\rho)[d(G/\rho)/dz]$$
$$= -(G/2)[d(G/\rho)^2/dz]. \quad (15)$$

Equation (15) can be employed to calculate the depressurization rate Σ along the nozzle configuration as follows:

(i) A first approximation to the critical flow rate G_c is obtained by neglecting the depressurization rate with time, Σ, or taking $\Sigma = 0$.

(ii) In carrying out this first approximation, several other values of higher pressures, P, would have been assumed and corresponding flows, G, and densities, ρ, would have been calculated. These combinations in values of P, G and ρ correspond to specific locations along the nozzle by realizing that the cross sectional area A there is obtained from

$$GA = G_c A_c = \text{constant}. \quad (16)$$

(iii) Next, values of Σ can be obtained for each local value of P along the nozzle from equation (15), and new values of ΔP_d, incorporating Σ, can be calculated for each such position and its pressure, P.

(iv) A new approximation to the critical flow rate can now be searched for from equations (10)-(12) employing the values of ΔP_d incorporating Σ every time a corresponding pressure P is assumed and the entire process repeated until the critical flow rate stabilizes.

The method described above adds considerable complexity to the computations, and it was decided instead to define an average value of Σ over the nozzle length, i.e. $\bar{\Sigma}$ is given by

$$\bar{\Sigma} = (1/\Delta z)\int_o^{\Delta z} \Sigma\,dz$$
$$= \tfrac{1}{4}(G_t + G_e)[(G/\rho)_t^2 - (G/\rho)_e^2]/\Delta z \quad (17)$$

where Δz refers to the nozzle length along the flow path. Equation (17) is an approximation to equation (15) with the subscripts t and e corresponding to throat and entrance conditions.*

If equation (17) is used, a single iteration will suffice for ΔP_d. For an initial value of ΔP_d calculated using the stagnation conditions, the throat pressure, P_t, to maximize the flow is obtained with the assumption of $\bar{\Sigma} = 0$. Then using $T_L = T_{f,P_t+\Delta P_d}$ a new ΔP_d is calculated and the process of maximizing the flow is repeated until ΔP_d stabilizes with a maximum flow rate of G_t. This value of G_t is used to calculate a new $\bar{\Sigma}$ and therefore a new ΔP_d, and the previous iteration process is repeated until G_t stabilizes. This technique is much easier to use but clearly is not as accurate as if one had tried to account for the point by point nozzle geometry as described earlier.

As noted before, an important element of the critical flow rate calculation is the expression for the decompression pressure drop ΔP_d. If enough critical flow tests had been performed where the void fraction was

* It has been suggested that the use of $\frac{1}{2}G_t^2[(G/\rho)_t^2 - (G/\rho)_e^2]$ may be just as appropriate at the critical or throat location.

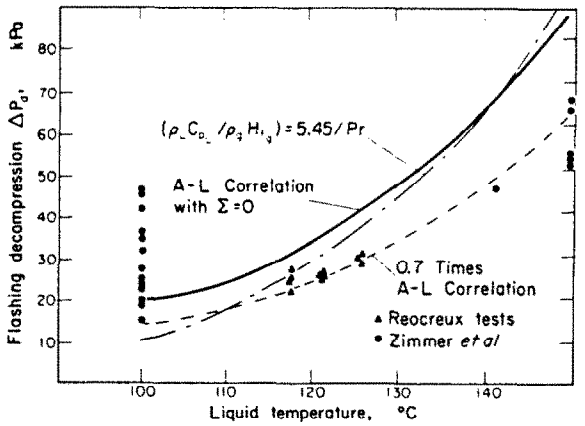

FIG. 3. Flashing decompression pressure drop vs. liquid temperature.

measured at the critical location, an empirical correlation for ΔP_d could be developed as illustrated in Figs. 1 and 2. Unfortunately, only the data of [1] and [2] provide such information consistently. However, they are limited to low steam-water pressure, and it was decided to employ equation (7) to assure high pressure coverage but to modify it with the data of [1] and [2]. For both [1] and [2], Σ and $\bar{\Sigma}$ are negligible and the calculated values of ΔP_d from the test data are shown in Fig. 3 together with equation (7) with $\Sigma = 0$. A curve corresponding to equation (9) with the exponent on the Reynolds number taken to be one is also plotted in Fig. 3. It is observed that the data of [1] and the data of [2], especially at increased pressure, can be represented well by multiplying the values of [3] by 70%. (It is interesting to note that in many of the tests of [9], the reported decompression pressure drop ΔP_d rapidly recovers to about 70% of the value given by equation (7) which specifies the decompression required to form the first bubble.) To minimize the impact of this 0.7 correction factor in the tests where Σ is large, the following expression was developed:

$$\Delta P_d = 0.258\sigma^{3.2} T_r^{13.76}(0.49 + 13.25\Sigma^{0.8})^{0.5}/(k_s T_c)^{0.5}(1 - \rho_g/\rho_L). \quad (18)$$

Equation (18) will satisfy the test results of [1] and [2] while not significantly disturbing the correlation of [3] when the parameter Σ is not negligible.

One final comment is in order before comparing the proposed model to available data. The calculations were performed using a computer program which requires the stagnation conditions and the nozzle entrance geometry as inputs. This program was developed by modifying the homogeneous equilibrium flow maximization portion of the computer code MASFLO by [14], which contains the 1967 ASME steam properties. In the process of searching for the critical pressure which maximizes the flow, the Hall computer program was modified to set a maximum for the assumed critical pressure. Under subcooled stagnation conditions, this maximum pressure, P_{max}, is set to satisfy the following conditions:

$$S_{L,\,P_{max}+\Delta P_d} = S_o \quad (19)$$

which ensures a minimum of zero quality at the throat. If the flow maximization results in

$$P_c = P_{max}$$

then the fluid remains all liquid and the critical flow rate is obtained by integrating the momentum equation (14) neglecting any changes in liquid density from the stagnation to the critical location, or

$$G_c = \sqrt{2\rho_o(P_o - P_{s,Ti} + \Delta P_d)}. \quad (20)$$

Equation (20) is identical to an expression proposed by both [12] and [13] except that they provide for the non-reversible pressure loss through the nozzle by means of a coefficient C_D in front of the square root. This approach is seen to be valid as long as there is no steam formation ahead of the nozzle throat.

Finally, it should be noted that the proposed model can be applied even with saturated stagnation conditions. Under the proposed flashing process, the water present in the stream is required to be decompressed an amount ΔP_d before additional steam is allowed to form. Under such conditions, the maximum pressure, P_{max}, is set to result in a quality at the throat, X^1, such that

$$(1 - X^1)H_{L,\,P_{max}+\Delta P_d} - X^1 H_{g,\,P_{max}} \leq H_o$$

As shown later, calculations have been performed under saturated stagnation conditions and the model predictions, as expected, fall slightly above the homogeneous equilibrium model.

COMPARISON OF MODEL TO TEST DATA

Let us first examine the validity of the presumed flashing process. Figures 1 and 2 already show that if the local pressure P is known then the local values of non-equilibrium steam quality and steam content can be predicted by the model. The same result is illustrated in Fig. 4 for one of the test results of [2]. In Fig. 4 from Zimmer *et al.*, there was critical flow, and the calculated throat pressure was found to be 12.3 K Pa compared to the measured value of 10.0 K Pa. Similar good correspondence was noted between predicted critical flow rate (24,160 kg/m^2 s) and measured critical flow rate (25,170 kg/m^2 s). Beyond the throat, the local steam quality was obtained from equation (12) assuming a constant throat pressure, typical of critical flow, in the diffuser. The liquid was kept at full non-thermal equilibrium and the steam voids were produced due to flow deceleration in the diffuser part of the test section. The predicted void fraction is shown in Fig. 4 compared to the measurements, and it is seen again that considerable non-equilibrium conditions prevail into the diffuser. If complete thermal equilibrium had been attained at the exit of the test section,

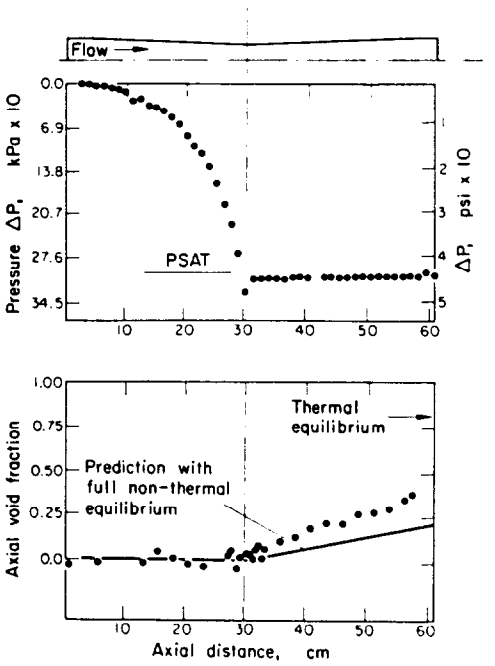

FIG. 4. Pressure and axial void fraction distributions in the Zimmer *et al.* test section.

the void fraction would be calculated to be 0.88 as shown in Fig. 4. In other words, in Fig. 4, steam is formed primarily due to the diffuser expanding geometry rather than reduced thermal non-equilibrium.

One of the major objectives of the newly developed model was to predict the large scale tests of Marviken. The Marviken experiments provide the only full scale data for critical flow with subcooled upstream conditions, and a simplified model which matches the test results would be quite useful in loss of coolant accident predictions. Figure 5 shows the critical blowdown rates for Run No. 24. The present model predictions are also plotted. It is observed that correspondence between model and tests is very good and superior to the homogeneous equilibrium model plotted on the same figure. In Fig. 5, three distinct regions of critical flow exist. In the highest flow rate region, water is present all the way to the critical location. In the intermediate region, very low steam quality and high non-thermal equilibrium prevail. This region is characterized by rapidly declining flow rates. In the third and last region, the critical flow rate is nearly constant, the steam quality is increasing, and the degree of thermal non-equilibrium is reduced. In Fig. 5, as well as for other Marviken runs, the intermediate region is difficult to predict because it takes the form of a vertical line and its starting point is quite sensitive to experimental stagnation temperature measurements. This is illustrated in Fig. 5 by providing critical flow predictions on the assumption that the stagnation temperature is 3°C below the measured values. Considerable improvement is obtained in the transition region. Fortunately, this intermediate region occurs over a small time interval and its contribution to the total integrated loss of coolant over time is quite small. In other words, from a practical viewpoint, it is not so essential to be as accurate in the intermediate region as in the other two regions of Fig. 5.

Figures 6–10 give a comparison of the measured and predicted critical flow rates for a number of Marviken tests. The overall agreement is satisfactory and it is observed that:

(i) the model does a very good job for short exit lengths and it tends to be high at increased exit lengths. This is illustrated in Figs. 5–7, where, for a diameter of 500 mm, the model matches the data at $L/D = 0.3$, becomes slightly high at $L/D = 1.5$, and falls above the data at $L/D = 3.1$, with L representing the length of the test section after the contraction and D being the diameter. The same trend is found in Figs. 8–10 for a diameter of 300 mm and L/D values of 1.0, 1.7 and 3.7.

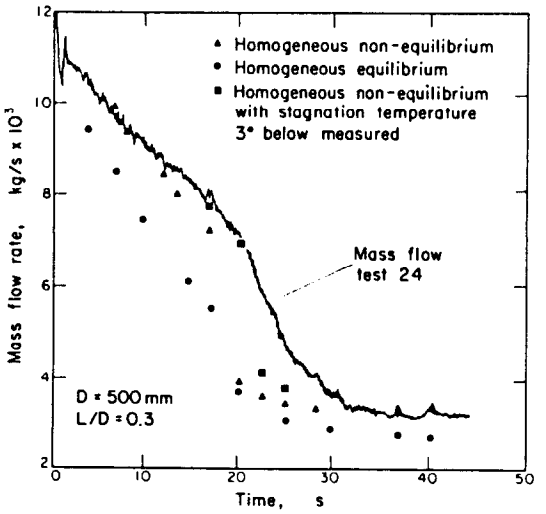

FIG. 5. Comparison of model to Marviken test 24 (D = 500 mm, L/D = 0.3).

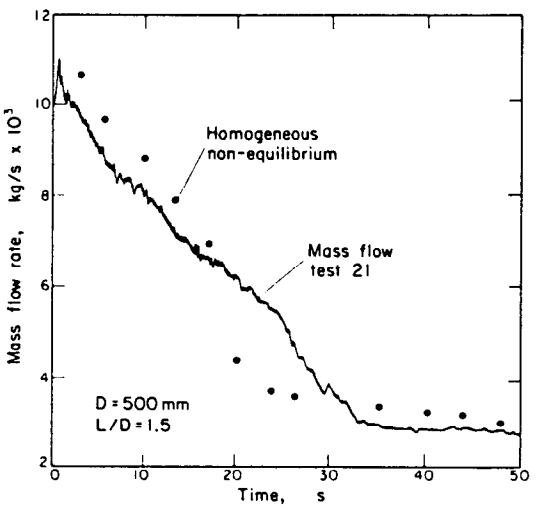

FIG. 6. Comparison of model to Marviken test 21 (D = 500 mm, L/D = 1.5).

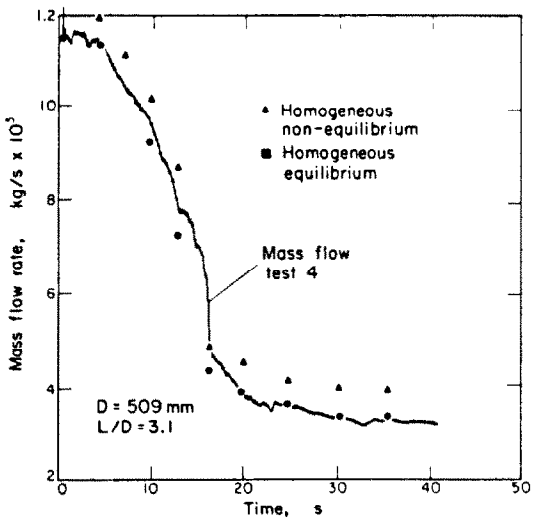

FIG. 7. Comparison of model to Marviken test 4 (D = 509 mm, L/D = 3.1).

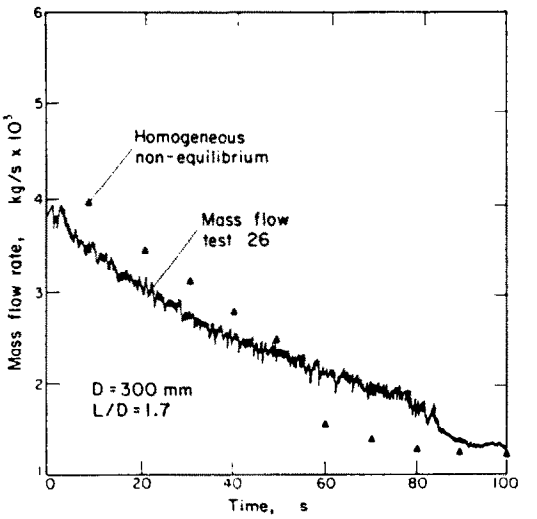

FIG. 9. Comparison of model to Marviken test 26 (D = 300 mm, L/D = 1.7).

Such over-prediction at high exit lengths is not unexpected since the model neglects any relaxation of mechanical non-equilibrium. This premise is supported by Fig. 7 where the homogeneous equilibrium model is seen to agree with the test data at L/D = 3.1. The benefits of relaxation are reduced in Fig. 10 at the increased value of L/D = 3.7 due to the reduced diameter of the test section in Fig. 10, i.e. the flow transit time after the contraction is less than in Fig. 7;

(ii) as noted for Fig. 5, the model underpredicts the test data in the intermediate region. This is noticeable in Figs. 5, 6 and 9;

(iii) the model tends to slightly overpredict critical flow during the blowdown and should be conservative. This is to be expected since the process was assumed to be isentropic (no friction) and relaxation of mechanical non-equilibrium was not permitted.

Table 1 and Figs. 11-13 give similar comparisons for the nozzle data of [2], [6] and [13]. The predictions are generally satisfactory and tend to support the validity of the proposed model. Table 1 gives excellent correspondence between the predictions and some typical measurements of [2]. Both the critical flow rates and the critical pressures are predicted well for all the subcooled runs in Table 1.

Figure 11 shows the model predictions and the subcooled data of Fincke [13]. The comparison is excellent. The predictions are slightly high, and this direction could be attributed to the lack of any discharge coefficient in the model. The correspondence

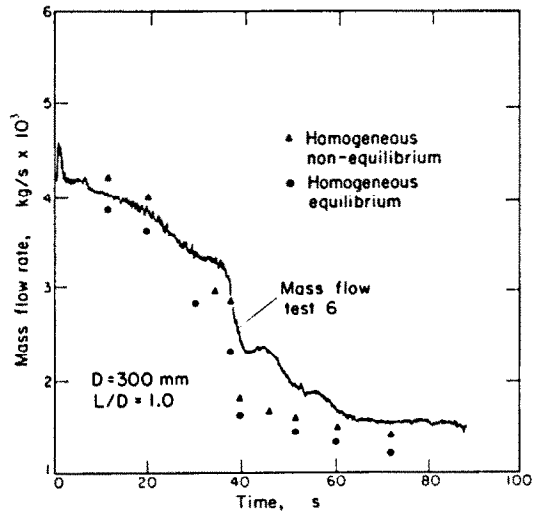

FIG. 8. Comparison of model to Marviken test 6 (D = 300 mm, L/D = 1.0).

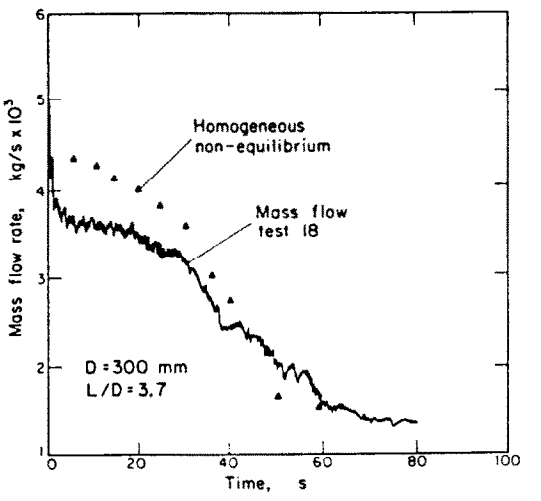

FIG. 10. Comparison of model to Marviken test 18 (D = 300 mm, L/D = 3.7).

Table 1. Critical flow rate and pressure prediction data from Zimmer *et al.* [2]

Test	P_0 (Psia)	T_0 (°F)	Measured mass flow rate (lbm/s)	Measured critical pressure (Psia)	Predicted mass flow rate (lbm/s)	Predicted critical pressure (Psia)
732	43.2	211	22.03	11.6	22.55	12.3
761	60.2	211	26.99	10.0	28.11	12.3
77	23.5	211	13.67	9.3	13.57	12.3
79	18.4	211	10.14	11.1	9.96	12.3
80	86.3	299	19.48	57.4	21.24	57.8
81	72.2	299	13.00	58.6	15.04	57.9

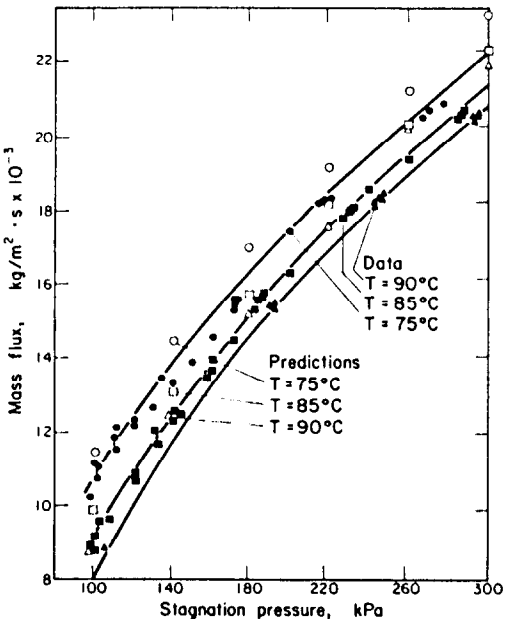

Fig. 11. Measured and predicted critical mass flux as a function of stagnation pressure for three isotherms for Fincke's nozzle.

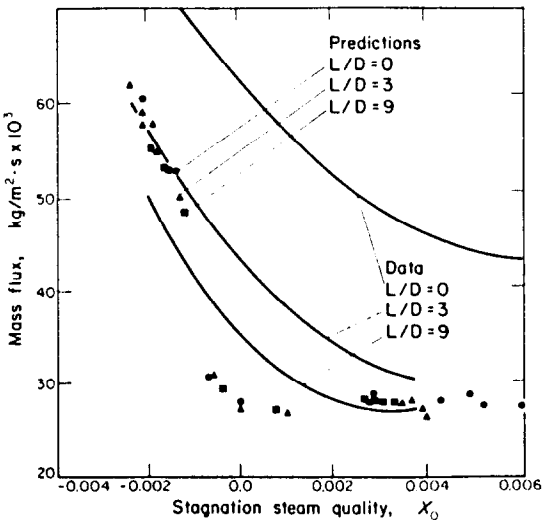

Fig. 12. Measured and predicted critical flow rates for nozzle 2 of Sozzi and Sutherland: P_0 = 900–1000 Psia.

between tests and model would improve considerably if the measured single phase discharge coefficient of 0.97 was employed.

In Fig. 12, the data from Nozzle 3 of Sozzi and Sutherland are plotted together with the model predictions. This configuration is very similar to the Marviken configuration and consists of a rounded nozzle followed by different length of tube. The primary difference is that the Sozzi and Sutherland [6] nozzle is at a much smaller scale and includes the configuration of $L/D = 0$. The test data and the model results are plotted for three values of L/D, i.e. $L/D = 0$, 3 and 9. The model predictions for L/D values of 3 and 9 were obtained by setting the average depressurization term Σ equal to zero and are the same for the two L/D values in excess of zero. It is observed that, except for the transition region, the model predictions are satisfactory at $L/D = 3$ and 9. The small difference in experimental values at $L/D = 3$ and $L/D = 9$ is due to friction which is not included in the model. At $L/D = 0$, the model tends to fall well below the data. It is important to note that, according to the proposed model, the decrease in critical flow rate with L/D is not only due to frictional losses, as others have reported, but also due to the fact that the depressurization term Σ or Σ decreases when a length of tube is provided after the nozzle. According to Fig. 12, the model may not be accounting properly for this change in depressurization rate as $L/D \to 0$.

Figure 13 shows a similar comparison with the venturi-type Nozzle 1 of Sozzi and Sutherland. The comparison between model and tests is good at subcooled conditions; as expected, it is poor in the transition region with the critical flow rate dropping too sharply with stagnation quality; and it is 20% low in the net steam generation region.*

* With two-phase stagnation conditions, there could be significant uncertainties in specifying the experimental stagnation enthalpy.

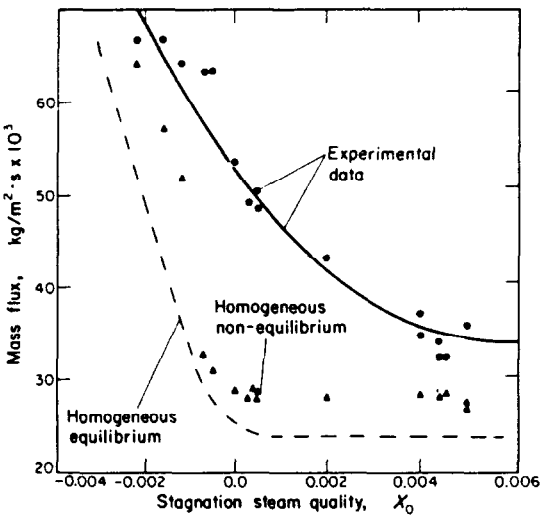

FIG. 13. Measured and predicted critical flow rates for nozzle 1 of Sozzi and Sutherland: $P_0 = 950$–1000 Psia.

There could be several explanations for the model under-predictions observed in Fig. 13 and in Fig. 12 at $L/D = 0$. One possible reason is that the assumed thermal non-equilibrium is too low. However, the good agreement between the model and the Marviken tests would not support such a contention. Another possible reason is the existence of 3-dim. effects and rarefaction waves being reflected downstream and interacting with the critical pressure. According to the authors and, as noted before, the most plausible explanation is that the depressurization rate parameter is not being properly accounted for. For the large scale tests of Marviken, Σ is small and negligible. The same is true for the low pressure and small scale condition of [2] and [13]. However, for the small scale and high pressure tests of [6], Σ starts to become important, except when the nozzles are equipped with exit pipes. For nozzles with exit lengths, $\Sigma \to 0$, the model again does very well. For Nozzle 2 with $L/D = 0$, it is suspected that the critical pressure position moves inside the contraction due to the sharp expansion at the throat. The same may be true, but to a lesser extent, of Nozzle 1. If this is the case, the value of Σ and Σ could be much greater than assumed, and it could account for the model predictions being too low. Another key reason for underestimating the role of depressurization rate is the use of the average parameter $\bar{\Sigma}$ instead of the local value, Σ, as noted when discussing equation (17). The parameter Σ is expected to be larger at the critical location than the average value proposed over the nozzle configuration since the velocity is the largest at that location and since there could be a substantial density change near the critical location. In summary, Figs. 4–10 reveal that:

(1) the proposed model predicts increased critical flow rates compared to the homogeneous equilibrium model. The differences between the two models are small when both models predict 100% liquid flow or when the vapor content is large at the critical location. However, the differences between the two models can become important in between these two conditions and the new model is substantially superior in that region;

(2) the basic assumption of maintaining the liquid in non-equilibrium conditions and not allowing it to relax is supported by the substantial relaxation times that could be inferred from the Marviken tests (see Fig. 7);

(3) the present model would predict no scaling impact except as it enters the depressurization rate, Σ. Since the depressurization rate is negligible for all nozzles at low pressure, according to the model, scaling will have a minimal role at low pressures. The same is true at all pressures for nozzles with exit lengths. The depressurization term, Σ, starts to become important at high pressure for nozzles with diffusers or no exit lengths. The model predicts increasing critical flow rates with decreasing scale in agreement with the test data trend. The tests, however, show a much greater increase than predicted and the deviation is amplified by the abruptness of the nozzle exit configuration. The proposed model needs further adjustment in this area to match such small scale tests;

(4) the model predictions fall too rapidly in the transition region between 100% liquid flow and equilibrium vapor flow. The deviation may be due to experimental uncertainties during this portion of the tests which is very limited in terms of time and overall blowdown flow;

(5) the model does not incorporate irreversible nozzle losses or frictional pressure drop and cannot consider any scaling effect associated with such mechanisms. For example, frictional pressure losses will be slightly higher at small scales. Furthermore, increased L/D values are employed usually at small scale which increases the role of friction.

EXTENSIONS OF PROPOSED MODEL

Three extensions of the proposed model are considered in [15]. They include:

(i) obstructions prior to the entrance of the nozzle;

(ii) irreversible loss in nozzle;

(iii) frictional losses in long test section after the nozzle.

CONCLUSIONS

(1) A critical flow rate model is developed for subcooled inlet conditions. The model assumes that the flow is homogeneous and that the liquid will flash to vapor when the liquid superheat exceeds a value specified in terms of pressure.

(2) The model gives good comparison with available data, especially when the contraction zone is equipped with a short constant area exit section.

(3) At high pressure and small scale conditions, the model under-predicts the data when the contraction

zone ends abruptly. The local depressurization rate becomes important in such circumstances and the model may not be accounting properly for it.

Acknowledgement—This work was prepared under EPRI Contract RP 1754-4. Their help is acknowledged gratefully.

REFERENCES

1. M. Reocreux, Contribution à l'étude des debits critiques en enoulement diphasique eau–vapeur. Ph.D. thesis, L'Université Scientifique et médicale de Grenoble (1974).
2. G. A. Zimmer, B. J. C. Wu, W. J. Leonhardt, N. Abuaf and O. C. Jones, Jr., Pressure and void distributions in a converging–diverging nozzle with non-equilibrium water vapor generation, BNL-NUREG-26003.
3. M. D. Alamgir and H. H. Lienhard, Correlation of pressure undershoot during hot-water depressurization, *J. Heat Transfer* (To be published).
4. D. Abdollahian, J. M. Healzer, E. Janssen and C. Amos, Critical flow data review and analysis: final report, S. Levy, Inc. EPRI Report NP-2192 (January 1982).
5. P. Saha, A review of two-phase steam–water critical flow models with emphasis on thermal non-equilibrium, BNL-NUREG-50907 (September 1978).
6. G. L. Sozzi and W. A. Sutherland, Critical flow of saturated and subcooled water at high pressure, General Electric Report NEDO-13418 (July 1975).
7. H. J. Richter, Separated two-phase flow model: application to critical two-phase flow, EPRI Report NP-1800 (April 1981).
8. R. E. Henry and H. K. Fauske, The two-phase critical flow of one component mixtures in nozzles, orifices, and short tubes, *J. Heat Transfer* **93**, 179–187 (1971).
9. G. S. Borkar, J. H. Lienhard and M. Trela, A rapid hot-water depressurization experiment, EPRI Report NP-527 (December 1977).
10. M. Alamgir, C. Y. Kan and J. H. Lienhard, An experimental study of the rapid depressurization of hot water, *J. Heat Transfer* **102**, 433–438 (1980).
11. O. C. Jones, Jr., Flashing inception in flowing liquids, BNL-NUREG-51221 (April 1980).
12. N. Abuaf, O. C. Jones, Jr. and B. J. C. Wu, Critical flashing flows in nozzles with subcooled inlet conditions, Paper presented at the Symposium on Polyphase Flow and Transport Technology, San Francisco, California, 13–15 August 1980.
13. J. R. Fincke, The correlation of non-equilibrium effects in choked nozzle flow with subcooled upstream conditions, ANS Small Break Specialists Meeting, Monterey, California, August 25–27 1981.
14. D. G. Hall, A study of critical flow prediction for semiscale Mod-1 loss of coolant experiments, INEL Report TREE-NUREG-1006 (December 1976).
15. S. Levy and D. Abdollahian, Homogeneous non-equilibrium critical flow model, EPRI Report (To be published).

MODELE D'ECOULEMENT CRITIQUE HOMOGENE ET HORS D'EQUILIBRE

Résumé—Un aspect important de la sûreté du réacteur à eau légère est la capacité de prévoir le débit massique maximal (ou critique) dans une fissure du circuit primaire. Durant les premiers instants d'un tel incident, l'eau est sous-refroidie ou légèrement saturée et des conditions sensibles de non équilibre existent, l'eau étant surchauffée au-dessus de la température de saturation. Il n'y a pas actuellement un seul modèle pour l'écoulement critique qui considère les conditions sous-refroidies en aval et le déséquilibre thermodynamique et qui soit valable pour une variété de configurations.

On développe ici un modèle simple de détente hors d'équilibre. Le modèle qui est applicable spécialement aux pressions décroissant rapidement le long du parcours suppose que l'eau est surchauffée (ou décomprimée) d'une valeur prescrite avant de se détendre en vapeur et que, à une pression locale donnée au-dessous de la pression de décompression, se forme assez de vapeur pour amener la surchauffe d'eau jusqu'à la valeur de décompression. De plus, l'écoulement est supposé homogène c'est-à-dire que la vapeur et le liquide ont la même vitesse. Enfin un processus isentropique est employé pour calculer la qualité de la vapeur hors d'équilibre et le débit critique.

Le modèle proposé décrit de façon satisfaisante les essais de dépressurisation et de débit critique par Reocreux [1] et Zimmer *et al.* [2], avec mesure des pressions locales et des fractions de vide. Un bon accord global est aussi obtenu avec les essais à grande échelle de Marviken, et la plupart des autres expériences à petite échelle. Le modèle ne peut pas rendre compte convenablement de l'effet de la dépressurisation sur les conditions de non-équilibre et il tend à sous-évaluer les essais à petite échelle avec forte pression quand la zone de contraction n'est pas suivie par une longueur de section droite constante.

Un élément clé du modèle est la chute de pression de décompression du liquide ou la surchauffe employées dans ce modèle. On montre qu'il est semblable à l'expression semi-empirique d'Alamgir et Lienhard [3], et une petite modification de leur expression est développée à partir des références expérimentales [1] et [2].

EIN MODELL FÜR HOMOGENE KRITISCHE NICHT-GLEICHGEWICHTS-STRÖMUNG

Zusammenfassung—Ein wichtiger Aspekt der Sicherheit bei Leicht-Wasser-Reaktoren ist die Möglichkeit, den maximalen (oder kritischen) Massenstrom aus einer Bruchstelle oder einem Leck im Primär-System zu berechnen. In der frühen Phase eines derartigen "blowdown" ist das Wasser unterkühlt oder leicht gesättigt, wobei ausgeprägte Nicht-Gleichgewichts-Bedingungen vorhanden sind; beispielsweise ist das Wasser über die Sättigungstemperatur überhitzt. Derzeit liegt nicht ein einziges brauchbares Modell für die kritische Strömung vor, das unterkühlte Verhältnisse und thermisches Nicht-Gleichgewicht der Zuströmung berücksichtigt, und das für verschiedene Anordnungen gültig ist. In dieser Arbeit wird ein vereinfachtes Nicht-Gleichgewichts-Modell für die Entspannungs-Verdampfung entwickelt. Das Modell ist speziell für solche Fälle anwendbar, in denen der Druck entlang des Strömungsweges rasch abfällt. Dabei wird vorausgesetzt, daß das Wasser um einen bestimmten Betrag überhitzt (oder dekomprimiert) werden muß, bevor es spontan verdampft und daß bei einem vorgegebenen örtlichen Druck unterhalb des Dekompressions-Druckes genügend Dampf gebildet wird, um die Überhitzung des Wassers auf den Dekompressions-Betrag zu senken. Darüber hinaus wird die Strömung homogen angenommen, d.h. Dampf- und Flüssigkeits-Geschwindigkeit sind gleich. Schließlich wird eine isentrope Zustandsänderung angenommen, um den Dampfgehalt bei Nicht-Gleichgewichts-Bedingungen und den kritischen Massenstrom zu berechnen. Es hat sich gezeigt, daß das vorgestellte Modell für die Entspannungs-Verdampfung die Versuche befriedigend beschreibt, bei denen Reocreux [1] und Zimmer u.a. [2] Entspannung und kritische Strömung untersucht sowie den örtlichen Druck und Dampfgehalt gemessen haben.

Gute Gesamt-Übereinstimmung ergab sich auch mit den Versuchen von Marviken im Original-Maßstab und mit den meisten Modell-Versuchen. Mit dem Modell läßt sich die Auswirkung der Entspannungs-Geschwindigkeit auf die Nicht-Gleichgewichts-Bedingungen nicht berechnen, und es neigt dazu, bei hohen Drücken gegenüber Modell-Versuchen zu kleine Werte zu liefern, und zwar dann, wenn hinter der Verjüngungs-Zone kein Abschnitt mit konstantem Querschnitt folgt. Wesentliche Elemente des Modells sind Druckabfall oder Überhitzung bei der Dekompression der Flüssigkeit. Es zeigt sich eine Ähnlichkeit mit der halbempirischen Korrelation von Alamgir und Lienhard [3], die auf der Grundlage der Daten aus [1] und [2] leicht modifiziert wird.

МОДЕЛЬ ОДНОРОДНОГО НЕРАВНОВЕСНОГО КРИТИЧЕСКОГО ПОТОКА

Аннотация — Важным аспектом обеспечения безопасности работы реактора с водным замедлителем является возможность прогнозирования максимального (или критического) массового расхода жидкости, обусловленного прорывом или утечкой в первичном контуре. На первых стадиях возмущения реактора отмечается недогрев воды или небольшое насыщение и возникают значительные неравновесные условия, например, вода нагревается выше температуры насыщения. Пока не предложено какой-либо адекватной модели критического потока, в которой учитывались бы условия недогрева вверх по течению, а также термическая неравновесность, и которая была бы справедливой для целого ряда конфигураций.

В работе предложена упрощенная неравновесная модель мгновенного испарения, которая может использоваться особенно в случае внезапного падения давления по длине канала. Модель основывается на предположении, что перед переходом в пар должен иметь место перегрев воды (или снижение давления) на заданную величину и что при заданном локальном давлении, величина которого ниже значения при декомпрессии, пар образуется в количестве, достаточном для того, чтобы перегрев воды мог снизится до декомпрессионного значения. Кроме того предполагается, что поток является однородным, т. е. скорости потоков пара и жидкости равны. И наконец, расчет неравновесного паросодержания и критической скорости потока проводится в предположении изэнтропичности процесса.

Показано, что модель мгновенного испарения удовлетворительно описывает опыты Рекрё [1], а также Циммера и др. [2] по снижению давления и критической скорости потока, в которых проводились измерения локального давления и объемного паросодержания. Получено также хорошее совпадение с результатами натурных испытаний Марвикена и большинством других лабораторных опытов. Модель не позволяет точно учитывать влияние интенсивности снижения давления на неравновесные условия и, как правило, дает заниженные значения в случае проведения лабораторных экспериментов при высоких давлениях, когда за зоной сужения канала не следует участок постоянного сечения. Основой модели служит предположение о падении давления жидкости или перегреве. Показано, что она аналогична полуэмпирической зависимости Аламжира и Линхарда [3], и предложена некоторая модификация этой зависимости на основе результатов работ [1] и [2].